CHAPTER IV

RESULTS AND DISCUSSIONS

In this chapter, the experimental results were reported and discussed, which divided into four main parts. Firstly, raw material characterization and preparation of mixed powders were given. Secondly, microwave and conventional combustion behavior of Al_2O_3-TiC powder were described in terms of type of precursors and heating methods. Next, the physical and mechanical properties of pressureless sintered Al_2O_3-TiC composites prepared form conventional and microwave combusted powders were compared and discussed. Finally the feasibility of microwave sintering was revealed.

4.1 Raw Materials and Mixed Reactant Characterization

The characteristics of raw materials including density, surface area and particle size were determined as shown in Table 4.1.Particle size distribution of raw materials given in Appendix B. The morphologies of raw materials characterized by SEM are shown in Fig 4.1. The phase analyses of raw materials are confirmed by XRD as presented in Appendix C. The XRD patterns demonstrate a clearly crystal structure of rutile, anatase and aluminum. In case of carbon, graphite is the only phase which can be detected as crystal phase while carbon black and activated carbon show patterns of amorphous phase.

Table 4.1 Raw materials characterization.

Raw material	Density (g/cm^3)	Particle size[d(4,3)] (μm)	Surface area (m^2/g)
Rutile	4.73	1.24	3.24
Anatase	4.04	0.36	11.17
Aluminum	2.99	11.99	0.59
Carbon black	2.12	1.13	9.23
Graphite	2.42	6.61	12.23
Activated carbon	2.99	41.75	1120.00

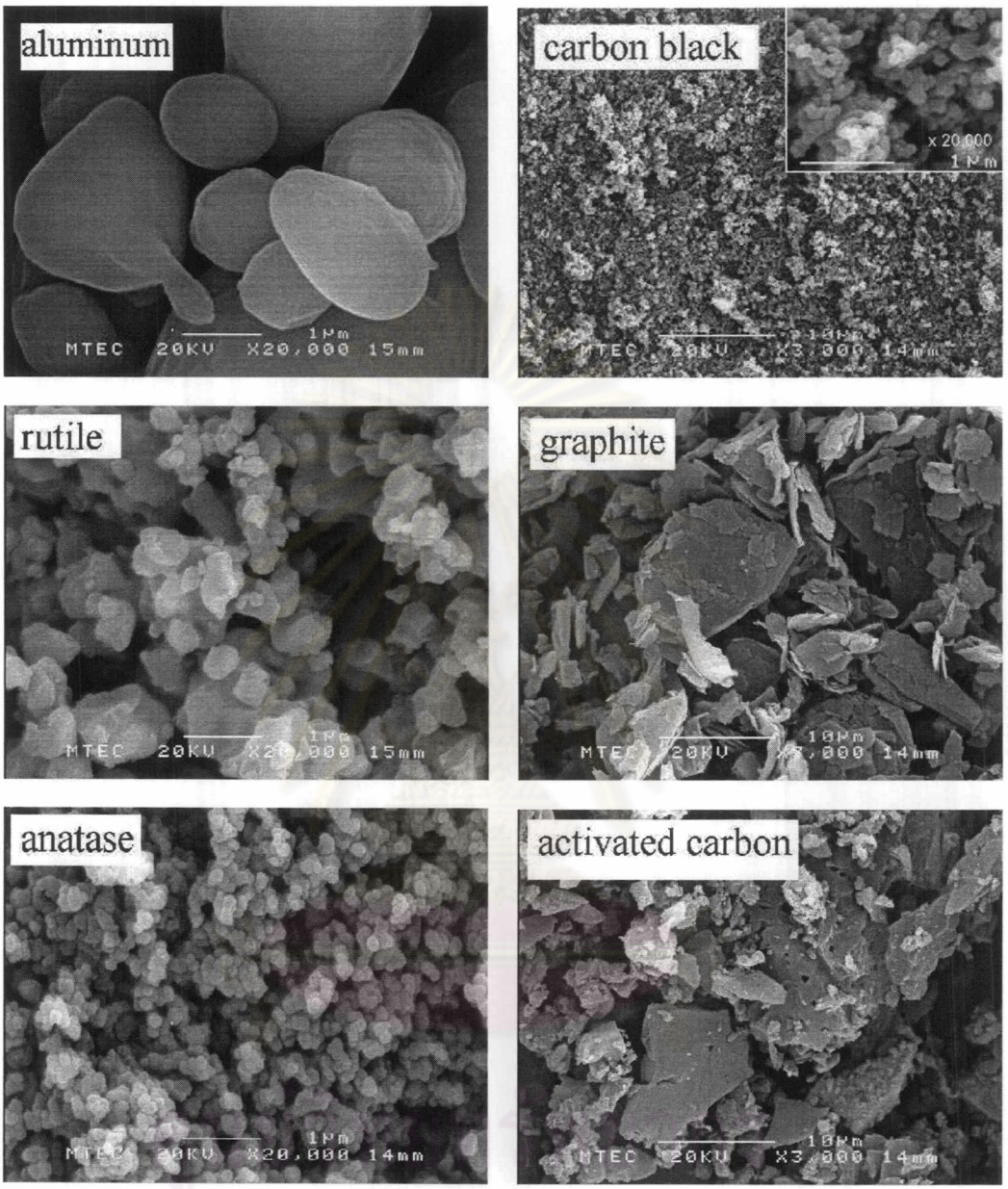

Fig. 4.1 SEM micrographs of reactant materials.

After mixing process, the particle size analysis of reactant mixtures were performed as shown in Fig. 4.2. The mixed powders with rutile as a precursor tended to form broader size distributions particularly in TC1 and TC3, while TC2 powders show a bimodal distribution. The peak distributions corresponded well with the sizes of precursors used. Unlike anatase precursor group, all mixed powder (TC4, TC5, and TC6) clearly exhibited bimodal size distribution. Ninety percent of the particles are

between 0.1 – 1 μm, distributed around the first peak, at about 3 μm. These particles are mainly anatase particle, except for TC4 mixture where small carbon black are well dispersed with anatase. Ten percent of the particle, however, fell in the 3 - 40 μm size range which distributed at the second peak

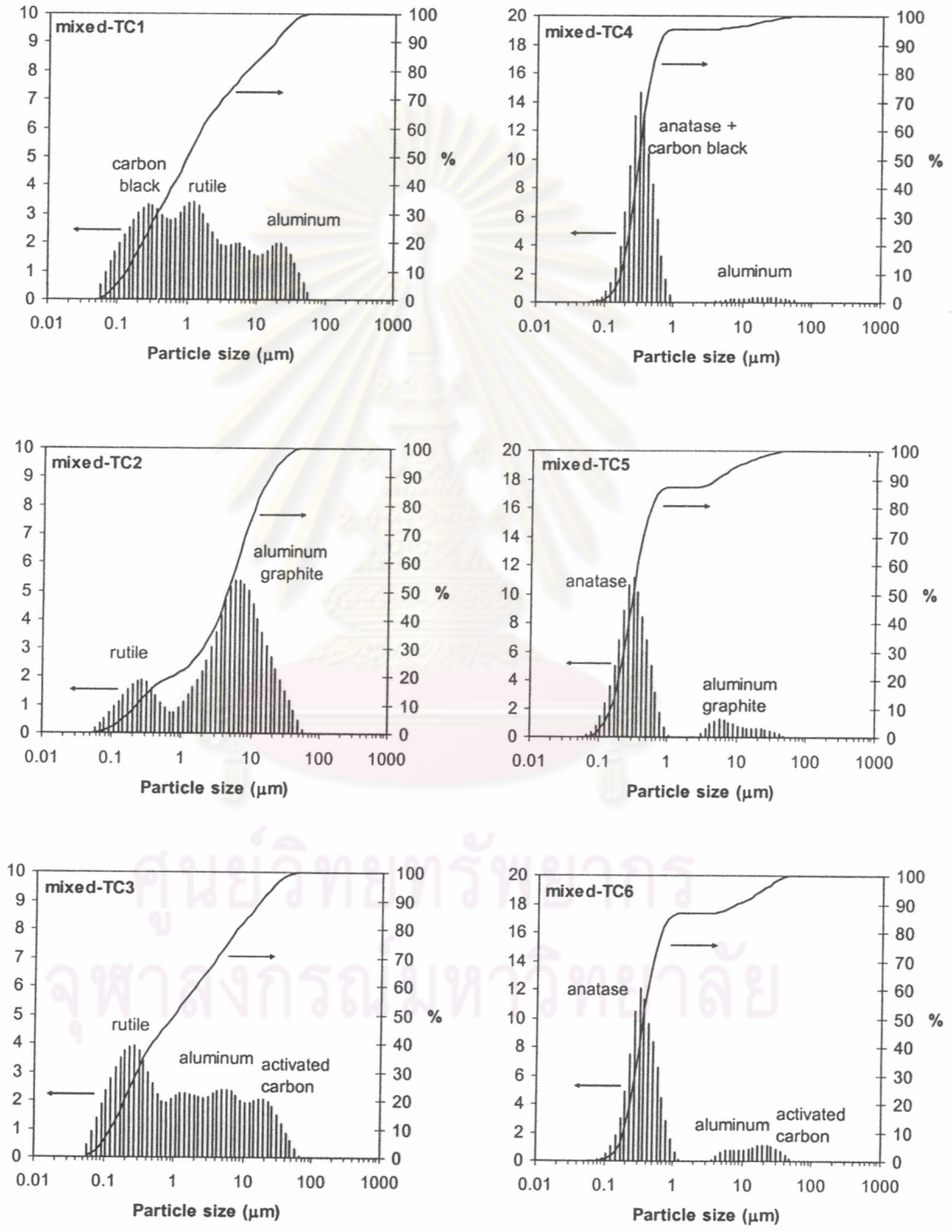

Fig. 4.2 Particle size distribution of mixtures with various TiO_2 and C sources.

4.2 Part 1: Combustion Synthesis of Al_2O_3-TiC powders

4.2.1 Characteristics and Microstructures of As-combusted Powder Products

The adiabatic temperature (T_{ad}) is used as an indication whether the synthesis of materials can be accomplished by a combustion synthesis (SHS). The adiabatic temperature of Al_2O_3-TiC calculated using thermodynamic data is 2330.98 K in the case of using rutile as a precursor and 2331.26 K for anatase. Therefore it could be assumed that the SHS reaction would be possible.

As evidenced in Fig. 4.3, Al_2O_3-TiC powders were successfully synthesized by conventional and microwave heating. It was found that all of reactant mixtures in microwave process were rapidly ignited more than ten times faster than conventional process. These results will be discussed more in details in a following section (4.2.2) The conventional samples were combusted in the explosion made thus it was found to be more violent than microwave. With a slow heating rate of 5^{o}C/min, the entire sample is heated uniformly to the ignition temperature and the reaction occurs simultaneously through the whole sample.

As for microwave heating, the samples were combusted in self propagating mode where initially ignited near the center at several locations and then propagated outwardly. The explanation might be that the heat generating in the sample might occur mainly where carbon, the highly microwave absorber material, homogeneously distributed in the sample. As carbon absorbs microwave energy, the heats rapidly transfer to the other reactants and ignition occurs. The sequential reaction proceeded in there stages: melting of aluminum, aluminothermic reduction of TiO_2 and finally TiC synthesis [32].

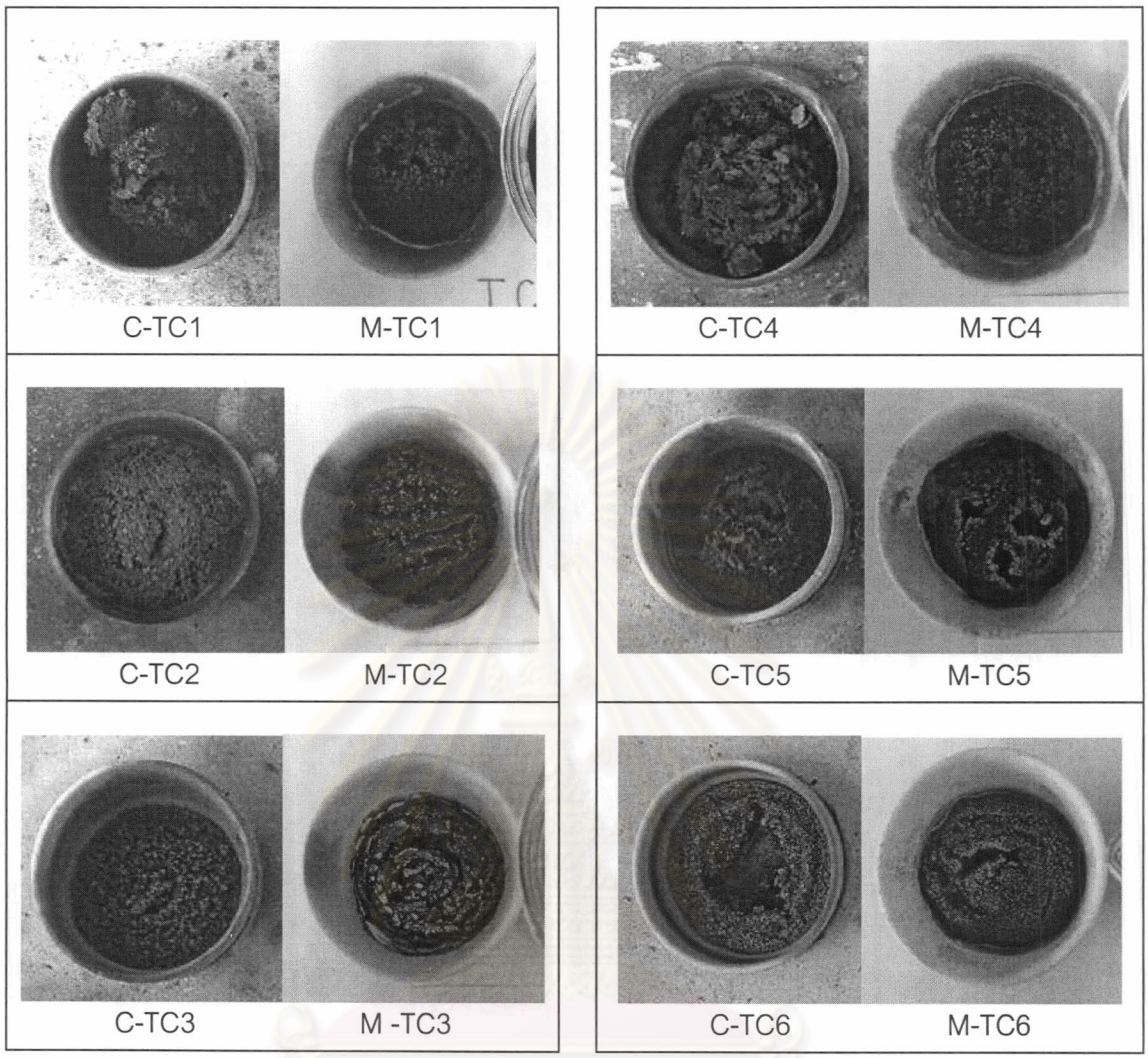

Fig. 4.3 As-combusted Al_2O_3-TiC powder by conventional and microwave heating.

In addition, it was found that combustion velocity in microwave and conventional combustion process depended mainly on carbon source than titania. Reactant mixtures with carbon black as carbon source (TC1 and TC4) provided the most violent exothermic reaction and the combustion immediately occurred in less than 1 sec, whereas the mixtures with activated carbon gave slower combustion rate about 2 - 4 sec. Moreover, it was obviously seen in conventional samples TC1 and TC4, that the highly combustion rate resulted in scattered product.

All as-combusted powders were fragmented and angular shaped and appeared largely in agglomerate forms which could be broken down in milling. However, more densified powders and a greater size of agglomerate were observed in

conventional combusted powders. This was though to occur because it took longer time than microwave process therefore a liquid phase would probably present in the powder products for longer periods.

The corresponding microstructures of these composites are given in Fig. 4.4. The product consisted of the fuse and interconnected structure and spherical particle which were confirmed to be Al_2O_3 and TiC respectively, by the EDS analysis. The Al_2O_3 partcles appeared to be interconnected relatively more than TiC particles because the liquid Al in filtrated and formed aluminothermic reaction with TiO_2. The morphology of TiC particles would attribute to the carbon source as reduced Ti reached with free C later on.

In addition, it was found that Al_2O_3 in conventional products are more continuously phase and large in size as compared with microwave products. The explanation may be because of the long dwelling time in conventional process, thus Al is completely melted when react with TiO_2 phase. Another explanation might be because the combustion temperature in this thermal explosion mode might exceed the melting point of Al_2O_3 ($2050^{o}C$), though it could not be detected by the thermocouple. Unlike conventional ignition, a finer Al_2O_3 grain size exhibited due to a shorter ignition and processing time in microwave process.

It was also observed that the TiC morphology and particle size are not quite different from original carbon source and not much influenced by combustion method neither conventional nor microwave process. However, it is interesting to note that the large TiC particle size is observed due to an agglomeration of C particles especially when a very small size of carbon black was used, as seen in the C-TC1 product.

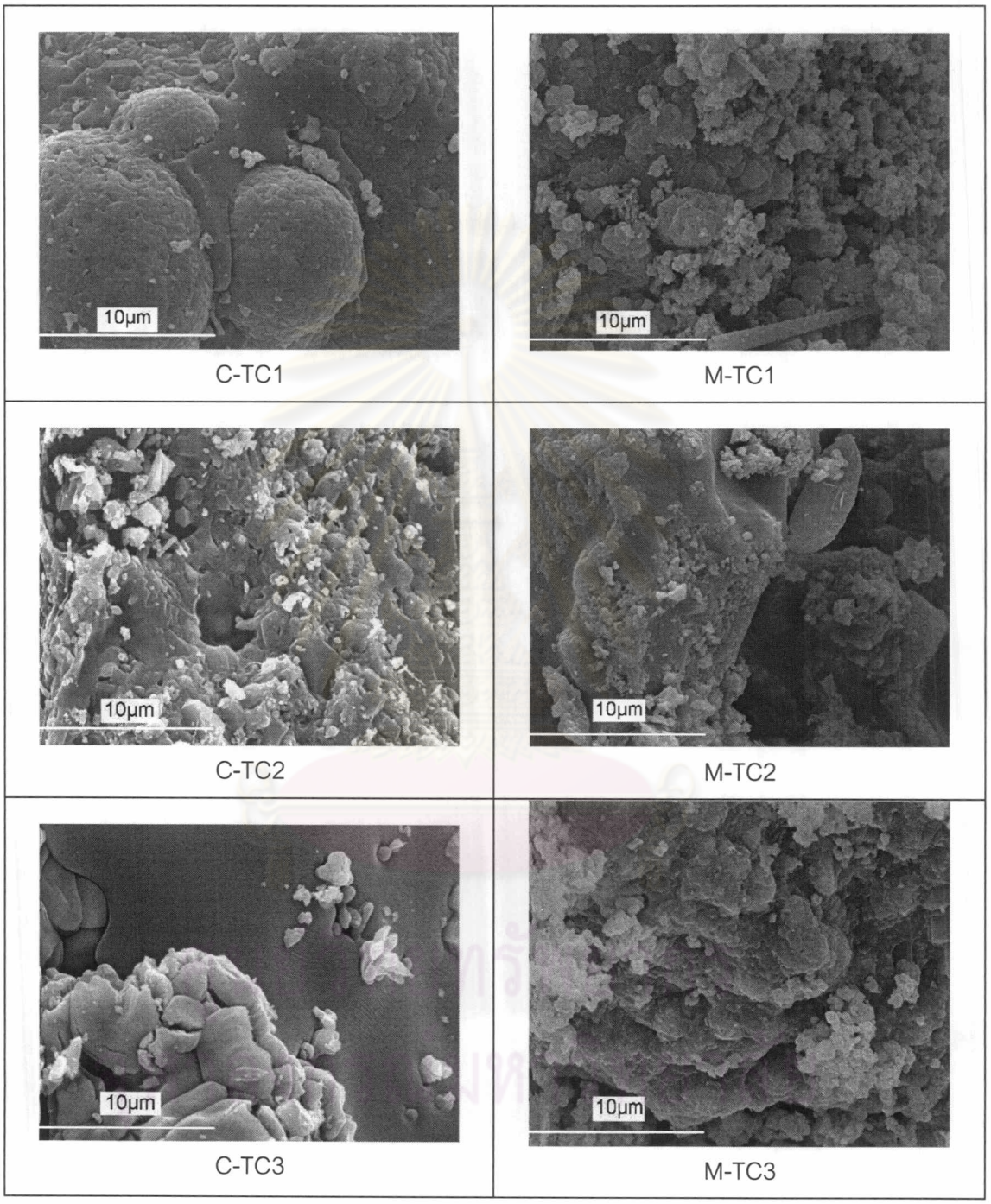

Fig. 4.4 (a) SEM micrograph of as-combusted agglomerate powders with rutile as titania source.

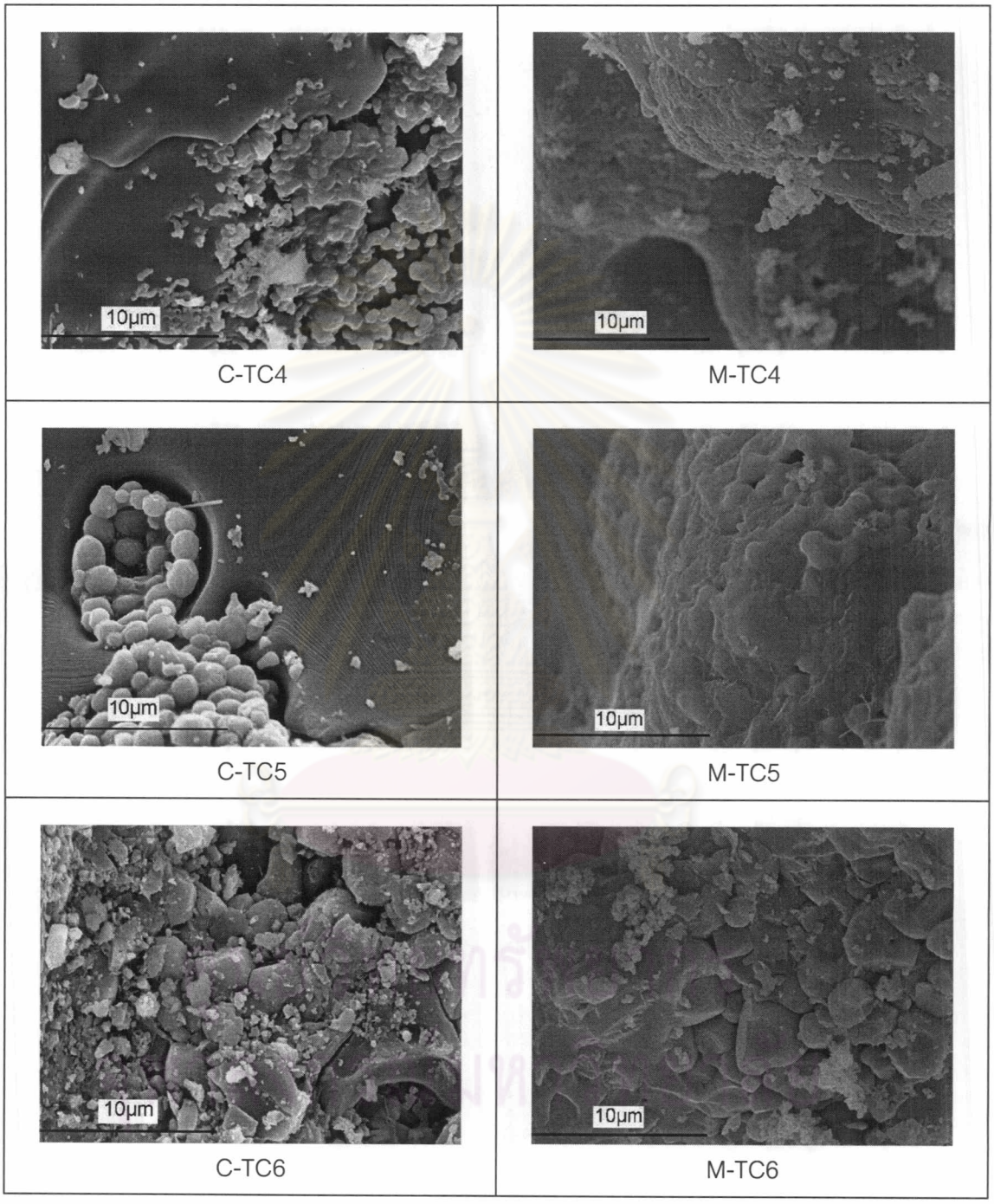

Fig. 4.4 (b) SEM micrograph of as-combusted agglomerate powders with anatase as titania source.

4.2.2 Combustion behavior

The data on the ignition time (t_{ig}), ignition temperature (T_{ig}), and also combustion temperature (T_c) of reaction were collected. Ignition time (t_{ig}) is a period of time since heat starts to raise the temperature of the reactants until ignition take places. Ignition is indicated by a shape rise in temperature, while the extremely high temperature achieves in a very short time (~1 to 3 sec) is called combustion temperature (T_c). Fig. 4.5 shows the microwave and conventional combustion behaviors of TC6 powders. The t_{ig}, T_{ig} and T_c of all powders combusted in conventional and microwave furnace are summarized in table 4.2

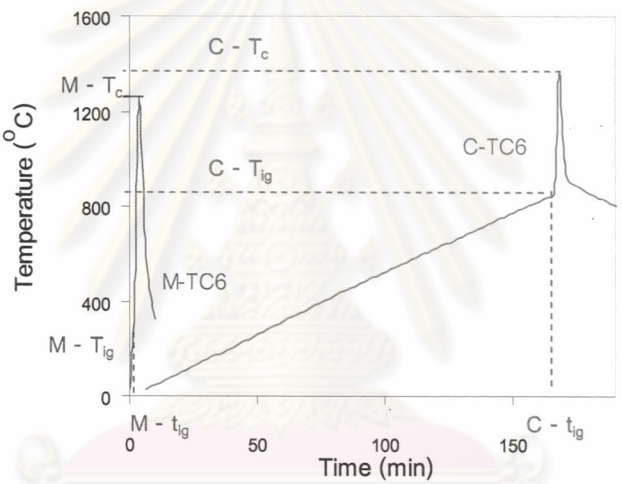

Fig. 4.5 The microwave and conventional combustion behaviors of TC6 powders

Table 4.2 Comparison of ignition time, ignition temperature and combustion temperature between conventional and microwave.

Composition	Ignition time, t_{ig} (min)		Ignition temp, T_{ig} (°C)		Combustion temp, T_c (°C)	
	C-TC	M-TC	C-TC	M-TC	C-TC	M-TC
TC1	172	0:40	891	305	1007	564
TC2	176	0:55	908	314	1077	819
TC3	159	1:54	826	329	902	1122
TC4	176	1:00	910	327	1050	960
TC5	175	2:33	906	331	1140	1089
TC6	165	2:58	859	365	1306	1255

It was obviously seen in Table 4.2 that all of the reactant mixtures in the microwave process were rapidly ignited compared to the conventional process. Ignition time of conventional combusted powders are about 159 -176 min while that in microwave process are less than 3 min.

4.2.2.1 Conventional combustion behavior

The temperature profiles of Al_2O_3-TiC powders with various TiO_2 and C sources ignited with conventional heating are demonstrated in Fig. 4.6. When compare between two groups of TiO_2 source, it can be seen that anatase (TC4, TC5, and TC6) seemed to take longer time for ignite than rutile (TC1, TC2 and TC3). It was suggested by T.D. Xia et al. that the combustion reaction would not completed unless the anatase-rutile transformation finished [47]. Samples containing anatase TiO_2 also shows a higher combustion temperature. This was contributed to a slightly higher exothermic and also higher thermal conductivity of anatase (0.148 $Cal.cm^{-1}.sec^{-1}.{}^{o}C^{-1}$) compared to rutile (0.430 $Cal.cm^{-1}.sec^{-1}.{}^{o}C^{-1}$) [48]. In addition, decreasing TiO_2 particle size increases contact area of particles and improves reaction kinetics.

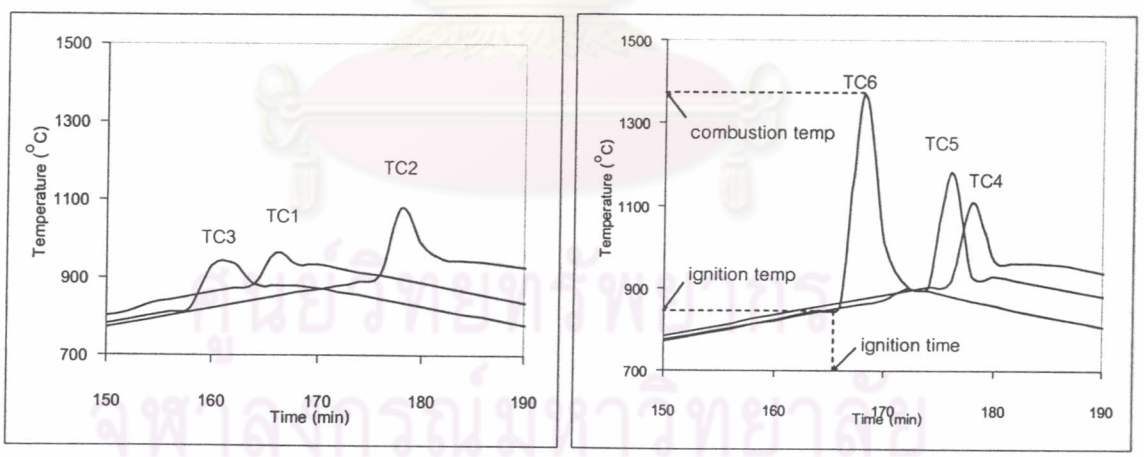

Fig.4.6 Temperature profiles during the conventional combustion reaction of (a) rutile precursor mixture and (b) anatase precursor mixture.

From Fig. 4.6, it was also observed that the mixture containing activated carbon (TC3, TC6) conventionally ignited fastest. The number of contact area between titania and aluminum plays an important role to the ignition time as previously explained

in sequence reactions as seen in equation 2.4 and 2.5. In anatase precursor mixture (Fig. 4.6(b)), slowest ignition time occurred when the carbon black which has the smallest particle size and low thermal conductivity was used (TC4). As shown in Fig. 4.7, small carbon black particle will form a continuous phase and act as a barrier to titania-aluminum particle contact, which is necessary for the initial aluminothermic reaction. However, when the carbon size is increased, the titania-aluminum particle contact is greater which may lead to decrease ignition time.

In addition, it can be seen in Fig. 4.6(b) that sample with smallest carbon particle size and highest surface area (TC4) had lower combustion temperature. This is presumably due to the reaction taking place over a longer time where heat losses become more significant. In contrast, the sample with the largest carbon particle size (TC6) was observed to have the highest combustion temperature. It was believed that a decrease surface area of the larger carbon particle size decreased heat loss.

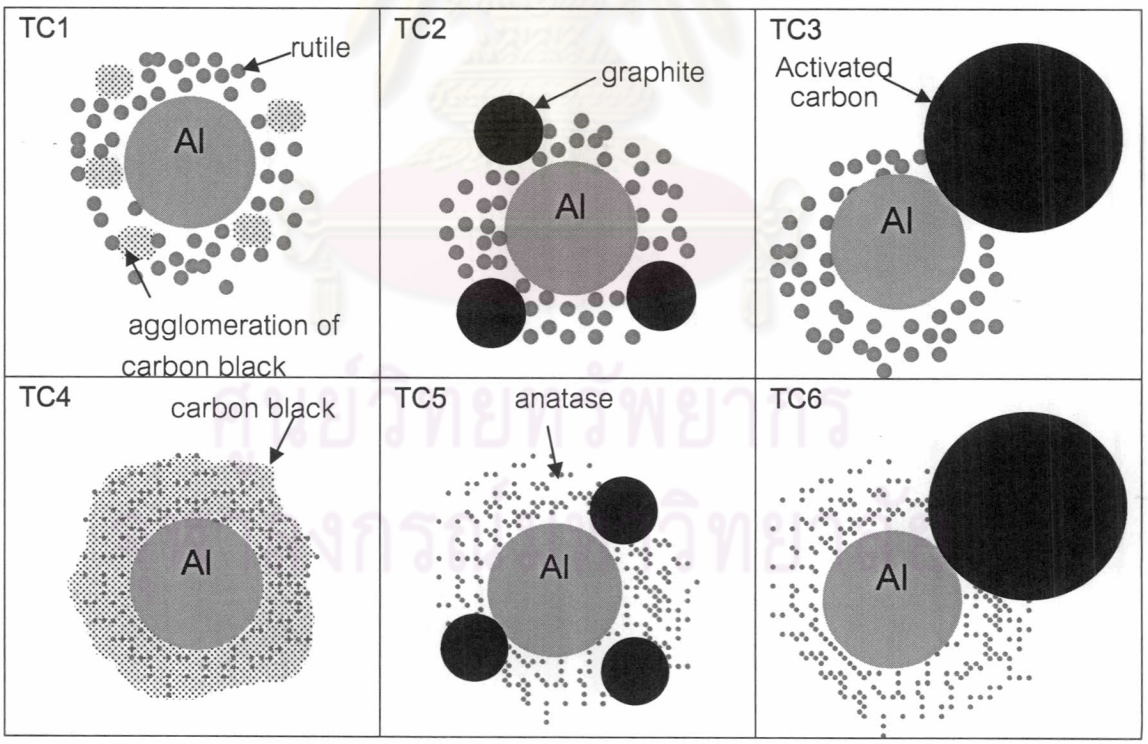

Fig. 4.7 Schematic showing particle packing in mixed reactant.

Fig. 4.6(b) also shows that the ignition time and temperature increased in the order of TC6, TC5 and TC4 sample while the combustion temperature decreased. In other words, the larger the difference between the initial and ignition temperature was, the lower the combustion temperature became. This was because more heat energy which generated from the reacted reactant powders was used in order to increase the temperature of adjacent reactant powder up to the ignition temperature.

The ignition behavior of sample with rutile showed less violent SHS mechanism compared to anatase, as earlier discussion concerned with its lower exothermic and adiabatic temperature. While the ignition time of the anatase system tended to increase with the decrease of the particle size of carbon, the dependency of ignition time of the rutile system on the size of carbon was more complicated (Fig. 4.6(a)). It was shown that while the fastest ignition also occurred with the sample containing a larger 45 μm activated carbon particle (TC3), those samples using carbon black (TC1) could be ignited faster than ones using graphite (C2) which was not observed in the case of anatase system. This was though to be because the carbon black might form a small agglomeration thus the inter-particle contact between titania and aluminum are not interrupted and still considerable to initiate alminothermic reaction. The agglomeration of carbon black was evident from the particle size distribution shown in Fig. 4.2. It was also confirmed by a large TiC particle size of synthesized TC1 powders illustrated in SEM micrographs in Fig. 4.4(a). In case of mixture with graphite (TC2), rutile particles may fill into the void between aluminum and graphit, thus resulted in longest ignition time. However, with a higher thermal conductivity of graphite particle, this mixture showed highest combustion temperature.

4.2.2.2 Microwave combustion behavior

The microwave ignition behaviors of various compositions are shown in Fig. 4.8. The ignition temperature of rutile as precursor group (TC1, TC2 and TC3) is 305, 314, 329 ^{o}C and anatase group (TC4, TC5, and TC6) are 327, 331 and 365 ^{o}C respectively. These are the surface temperature, which exhibited lower than that at the center of sample. In addition, it can be seen that the record combustion temperature

value, T_c, in these cases (600 -1300 ^{o}C) were very far from the adiabatic temperature because of the large amount of heat losses due to a large chamber size in microwave furnace.

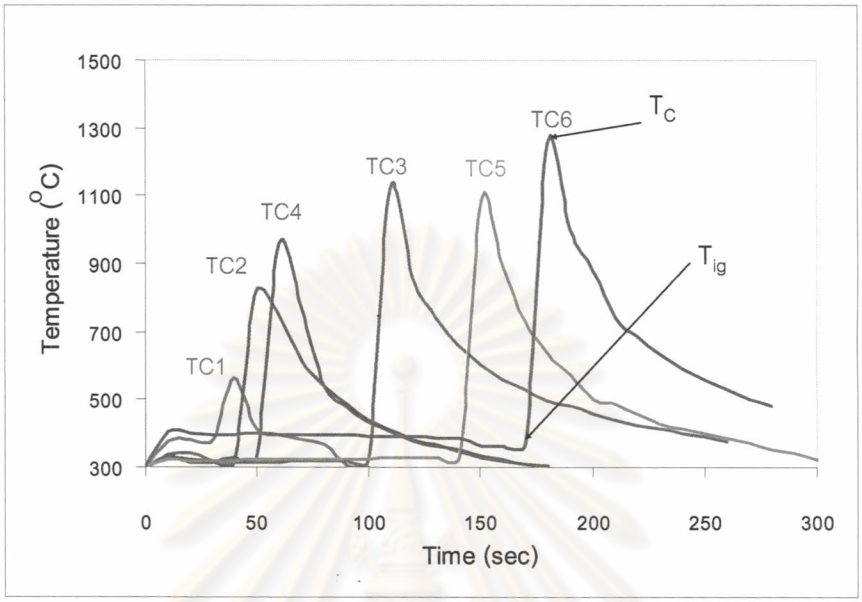

Fig. 4.8 Temperature profiles of the microwave combustion reaction

The microwave absorbtion ability of individual reactants is illustrated in Fig. 4.9. Ti can be seen that material with moderate electrical conductivity (C) heated more effectively than either insulating (TiO_2) or highly conductive (Al). As seen in Fig. 4.9, when exposed to microwaves, carbon black and graphite reached temperature of 900^{o}C and 700^{o}C, respectively within 40 sec, while activated carbon has a slow heating rate and attains highest temperature of only 600 ^{o}C. No temperature above 500 ^{o}C was recorded for Al powder. Low dielectric losses and low thermal conductivity sample, TiO_2, were difficult to heat from room temperature, even though microwave penetration was significant. The dielectric constant of anatase is lower than that of rutile, 114 and 48 respectively [48]. Thus it is heated less effectively than rutile, according to the equation relating dielectric properties to the power absorbed of material (equation2.20).

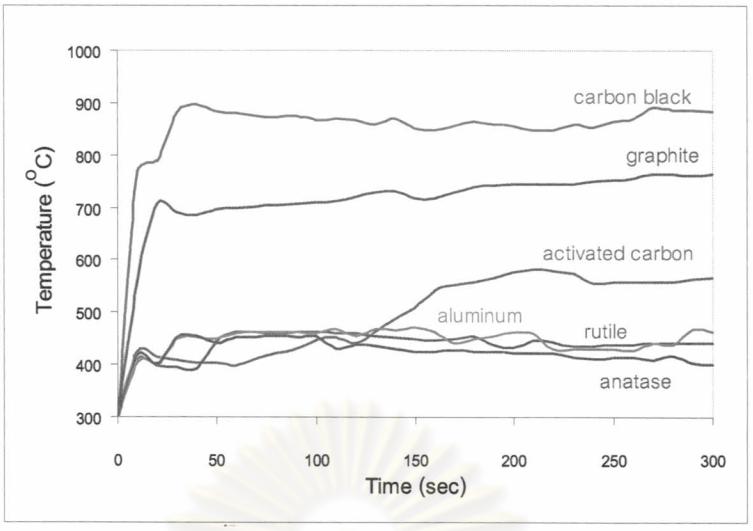

Fig. 4.9 Temperature profile of the reactants heated by microwave energy.

As seen in Fig 4.8, samples with anatase as TiO_2 source required longer time to ignite and thus gave higher combustion temperatures than ones with rutile. The increase in ignition time resulted in a large amount of heat accumulation and thus a high combustion temperature. This observation is in agreement with the thermodynamic calculation which indicated that the exothermic energy of the sample containing anatase is slightly higher than that containing rutile (Appendix A). In addition, when anatase (0.1μm) was used, it may be possible for a continuous anatase phase to act as a barrier between carbon-aluminum particle contacts. The heat transfer from carbon particle, highly microwave-absorbing material, to aluminum particle decreased. Thus it would take longer time for initial reaction between TiO_2 and Al to occur. Beside, a prolong ignition time of mixtures containing anatase can attributed to a lower in dielectric constant of anatase as aforemention.

It was also notice that, the microwave ignition behavior depends on carbon source, which is the main absorber precursor in these mixtures. As shown in Fig.4.9, carbon black heats more effectively than graphite and activated carbon. Comparing among carbon source, the mixture containing activated carbon (TC 3 and TC 6) would take the longest time to ignite and also showed the highest combustion temperature. The difference in particle size along with the ability to absorb microwave energy of these carbon sources plays a significant role in the ignition behavior. With a

higher purity and smaller particle size, carbon black can absorb microwave energy more efficiently compared to graphite and activated carbon, thus ignite fastest. Also as the carbon particle size decrease, it can be distributed in the mix reactants more uniformly, providing more contact area with other phases. There, heats generated from the smaller carbon particles transfers more rapidly to the other reactants resulting in a shorter ignition time

As seen in the mixtures containing rutile phase (TC1, TC2 and TC3), the one with rutile-carbon black ignited fastest. This may be because it provided the best reactant particle arrangements and particle contact between titania-aluminum which is believed to be the initial reaction during synthesis. When graphite was mixed with rutile, graphite particle size (6-7μm) was closed to Al particle size (7-15 μm), thus smaller microwave transparent rutile particles (1-2 μm) would be distributed among larger particles of both graphite and aluminum. This structure resulted in longer time. However, the mixture of rutile-activated carbon-aluminum was observed to have the longest ignition time. A possible explanation for this was that the heat generated within activated carbon (45 μm) was competed between aluminum and rutile phase. The same trend has also found in the mixtures containing anatase phase (Tc4, TC5 and TC6).

Nevertheless, all of reactant mixtures in microwave process were rapidly ignited more than ten times faster than conventional process. The ignition times required for microwave process samples containing (TC1-TC3) and anatase (TC4-TC6) were approximately 40, 55, 114 sec and 60, 153, 178 sec respectively. While the microwave-ignited powder could be achieved within 3 minutes, it would take about 3 hours to conventionally ignited samples (Table 4.2).

4.2.3 Physical Characteristics of Combusted Powder

After the combustion process, synthesized powder was milled by alumina ball (diameter 8 mm) in ethanol for 96 hr to reduce particle size and disperse agglomerate. The physical characterizations of synthesized Al_2O_3-TiC powders are presented as follow.

4.2.3.1 Phase Analysis of combustion products.

The confirmation of products phase was made by XRD as are shown in fig.4.10 (a) and (b). For TC1, TC2, TC4 and TC5 the XRD patterns indicated a complete conversion of reactant to Al_2O_3 and TiC product which were not different from the mixture of 53wt%Al_2O_3 – 47wt.%TiC commercial powder. The XRD pattern of product containing activated carbon, TC3 and TC6, revealed not only Al_2O_3 and TiC but also an Al-Ti-O metastable phase signal. The weak peak of metastable phase resulted in a decrease of main peak in the final product. The explanation might be because of impurity contained in activated carbon. Typically, very high temperatures are reached in exothermic reactions and all the volatile impurities evaporate producing high purity product. In this work, impurities from activated carbon and also a large amount of heat loss in the conventional and microwave chamber decreased combustion temperature down to a point that combustion reaction did not occurred completely and impurities in product TC3 and TC6 has remained. A further in-depth investigation is needed.

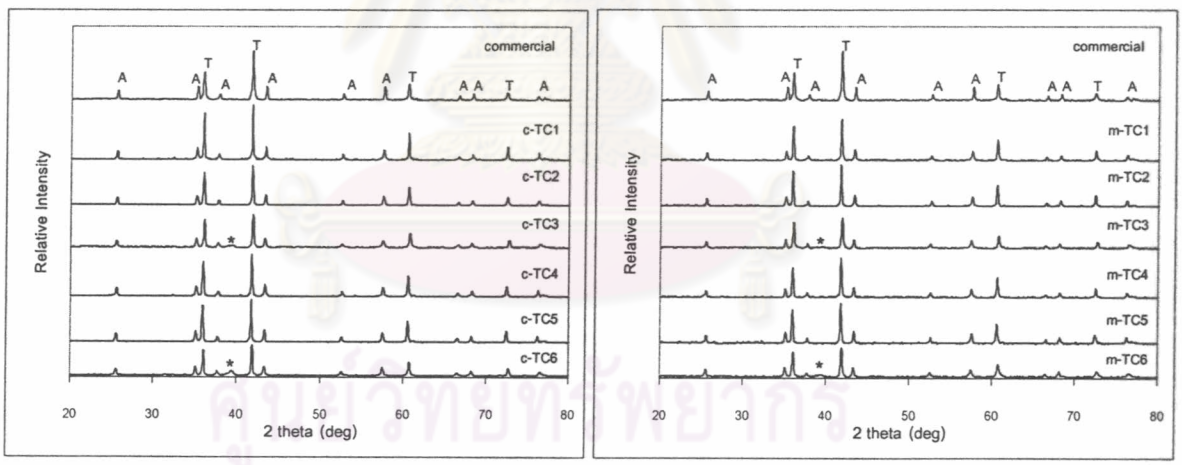

Fig. 4.10 XRD patterns of synthesized powders compared with mixed commercial powder: (a) conventional synthesized powders and (b) microwave synthesized powder (A=Al_2O_3, T=TiC, *=metastable phase)

4.2.3.2 Phase Conversion Determination

Quantitative phase analysis of mixtures of polycrystalline material is often difficult because there were many variables involved in determining the relative amount of each phase. The important variables are absorbtion coefficients, structure factor,

particle size and resolution of diffraction peak. Point of interests in the content combusted product is a ratio of Al_2O_3-TIC. A simple, fast and reproducible technique for the determination of phase content was developed from C.P.Gazzara and D.R.Messier's method [49].

Standard graph was made up from peak intensity of Al_2O_3 and TiC shown in XRD patterns of commercial mixture powders (Al_2O_3 and TiC) with various weight ratios. The phase conversions of synthesized powders (TC1-TC6) were then obtained by using each maximum peak height of Al_2O_3 and TiC phase given in XRD patterns. The calculation method is shown in Appendix D. The phase conversion of the reactant mixtures to Al_2O_3-TiC products were reported in term of percent of TiC as seen in Fig. 4.11. It was observed that the conversion of reactant is a function of particle size of carbon, which is the %TiC of combusted products was smaller as carbon particle size increased. It was though that with pure and smaller carbon black source, the combustion took place where reactants convert to product more completely compared to others.

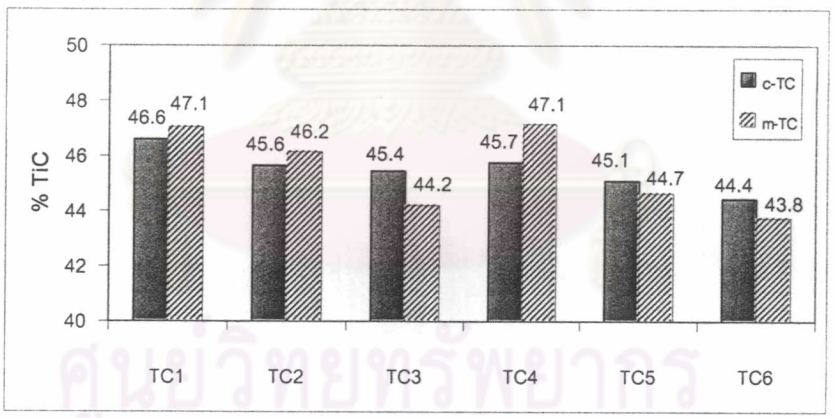

Fig. 4.11 Percent TiC in conventional and microwave combusted products calculated from the peak height obtained from XRD results.

4.2.3.3 Microstructure and Powder Characteristic

The corresponding microstructures of these milled-composite powders are shown in Appendix E. The powders were fragmented, angular shaped and still remained a lot of agglomerate. All compositions did not show any significant differences in morphology. The presence of aluminum, oxygen, carbon and titanium in EDS analysis

showed the consistent dispersion of Al_2O_3 and TiC phase as seen in Appendix E. The characteristics of ignited powders including particle size (d[4,3]) and surface are presented in Table 4.3. The particle size distribution of Al_2O_3-TiC synthesized powders by microwave and conventional heating are shown in Appendix F.

Table 4.3 Characteristics of conventional (C-TC) and microwave (M-TC) combustion synthesized Al_2O_3-TiC powders.

Batch	Density (g/cm^3)		Particle size (μm)		Surface area (m^2/g)	
	C-TC	M-TC	C-TC	M-TC	C-TC	M-TC
TC1	4.33	4.05	6.38	6.58	8.97	7.55
TC2	4.98	4.93	8.90	3.84	4.87	16.26
Tc3	4.80	5.07	9.88	3.29	3.41	6.31
TC4	5.10	5.18	8.80	7.50	4.44	4.09
TC5	4.95	5.04	9.79	5.28	3.99	9.64
TC6	4.56	5.18	4.36	9.22	4.30	3.60
Commercial	5.31		4.24		-	

Pycnometry analysis showed that the densities for all powder were in range of 4.04 – 5.18 g/cm^3. The densities of combusted powders were not quite different from the commercial mixture, while that of microwave combusted powders are closer to commercial value than conventional. The microwave products with anatase as tiania source (TC4-TC6) had a slightly higher density and particle size than those of rutile. One of the reasons might be because the higher combustion temperature resulted in a higher density of agglomerated powders that were too difficult to comminution by ball milled. The decrease of particle size corresponded to surface area, which is the small particle result in high surface area. The mean diameter of these combusted powders were in range of 3.29 – 9.88 μm with the largest size limited to less than 25 μm. These data show mostly the agglomerate sizes of product as corresponding with SEM micrographs.

In summary, microwave heating is fundamentally different from conventional processing in its heating mechanism. In conventional heating, heat was transfer from heating element to sample surface, and then conducted to the interior, therefore all reactant powders experienced the same temperature before ignition took place. In microwave heating, heat is generated within the sample itself by interaction of microwave with material. In this combustion reaction, the heat source occurred inside samples was mainly depend on microwave absorbtion efficiency of carbon source. TiO_2 particle is considered transparent to microwave, while Al particle reflect microwave; therefore heating was not occurred.

The different type of precursors affected the combustion behavior. Samples with anatase as TiO_2 source required longer time to ignite. This phenomenon was found in both case of convention and microwave combustion process. The thermodynamic consideration indicated that the exothermic of the sample containing anatase is slightly higher than that containing rutile. Carbon type gave a different effect in combustion behavior in conventional and microwave process.

In conventional combustion process, as the carbon size is larger or form an agglomeration, it leads to the reducing of ignition time due to it provides a greater number of contact area between titania and aluminum, which is necessary for the initial aluminothermic reaction. In addition to microwave process, a higher purity and smaller particle size of carbon played an important role to ignition behavior. Carbon black can absorb microwave energy more efficiently compared to graphite and activated carbon, thus ignite fastest. Also as the carbon particle size decreases, it can be distributed in the mix reactants more uniformly, providing more contact area with other phases. Therefore, heats generated from smaller carbon particles transfers more rapidly to the other reactants resulting in a shorter ignition time.

4.3 Part 2: Conventional Sintering

4.3.1 Conventional Sintering Without Additive

Pressureless sintering at 1900 ^{o}C was applied to study the sintering feasibility of microwave and conventional combusted Al_2O_3-47wt%TiC powders. The Vickers hardness of each composition is dependent on the relative density which calculated from bulk density, as shown in Fig. 4.12. The relative densities of pressureless sintered Al_2O_3-47wt%TiC composites prepared by conventional combustion synthesis (C-TC) are in the range of 92.6 – 95.8 %TD and that of pressureless sintered Al_2O_3-47wt%TiC composites prepared by microwave combustion synthesis (M-TC) are in the range of 84.8 - 96.8 %TD, while the hardness of C-TC and M-TC are 12.10 – 18.94 GPa and 6.81 – 15.58 GPa, respectively. The enumerations of these values are displayed in Appendix G.

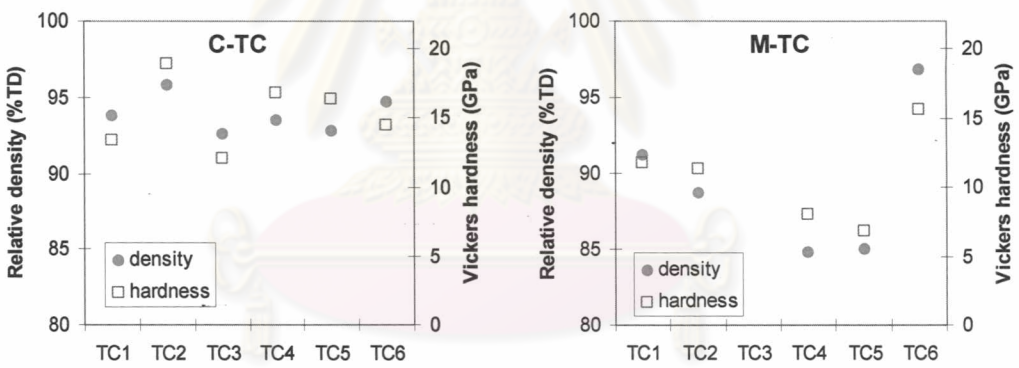

Fig. 4.12 The relative density and hardness of (a) conventional synthesize powders and (b) pressureless sintered of microwave synthesized Al_2O_3-47wt%TiC powders

It seemed that the ignition time and combustion temperature may have some influences on the density and hardness. In the sintered products of C-TC powders, the reason that C-TC2 and C-TC6 exhibited relatively higher density might be because C-TC2 took longer time to ignite while C-TC6 experienced the highest combustion temperature compared to the others. In addition, the sintered product of C-TC3 ignited fastest; as a result it provided low density and hardness. It was thought that the metastable phase, which was detected by XRD, led to the increasing of gas generation of reaction between Al_2O_3 and TiC during sintering at high temperature.

Although this metastable phase was also found in the sintered product of C-TC6, due to the highest combustion temperature occurred as shown in temperature profile in Fig. 4.6(b), a densified agglomerated powder was obtained which gave stability to the synthesized powders. In case of the pressureless sintered product of M-TC powders, the rising or dropping of hardness value also corresponds to the sintered density. However, it was found that both properties are lower than sintered product of C-TC powders as seen in Fig. 4.12(b). A great number of gas generation found in sintered product of M-TC3 made this pellet sample full of pore and become irregular shape, thus the density and hardness could not be attained.

The apparent porosity and water absorbtion of pressureless sintered product of both C-TC and M-TC powders are given in Table 4.4. These results are in good agreement with the density and hardness value that the properties of M-TC products are inferior. The obviously high apparent porosity let M-TC products decrease in relative density and hardness. It might be a reason that the processing time of conventional synthesis process was longer than microwave synthesis process considerably. The conventional synthesized powders were soaked at high temperature for a period of time and might become strong aggregate, thus it was difficult to break particle bonding between particles to generate gas. In contrast with microwave synthesized powder, the synthesis process was so fast such that, once ignited, the temperature was raised to combustion temperature and then cool down to room temperature within seconds. Therefore, the agglomerate of microwave synthesized powder was loosed and had more mobility to form reaction during sintering process.

Table 4.4 Apparent porosity and water absorbtion of the Al_2O_3-47wt%TiC sintered products.

Compositions		TC1	TC2	TC3	TC4	TC5	TC6
Apparent porosity (%)	C-TC	0.19	0.40	2.30	1.37	2.08	0.19
	M-TC	3.14	4.68	-	8.98	8.88	0.18
Water absorbtion (%)	C-TC	0.05	0.09	0.56	0.33	0.51	0.05
	M-TC	0.79	1.20	-	2.42	2.39	0.04

The microstructures of sintered products are exhibited in Fig. 4.13, where dark and light phase were confirmed to be Al_2O_3 and TiC phase, respectively, by EDS analysis. Each grain of TiC had a rather angular shaped and a size of less than five microns. Further, the TiC grains were interconnected. The sintered specimen from microwave and conventional combustion shows similar porous microstructure, these pores are mainly associated with the TiC grain. The adiabatic temperature of this reaction (~2331 K) exceeds the melting point of Al_2O_3 (~2030°C) but less than that of TiC (~3140°C). Therefore, it was thought that these pores are remained because TiC particles were difficult to densify. Another possible reason is the chemical reaction between Al_2O_3 and TiC occurred at high temperature, introducing pores into the composites which deteriorate the physical and mechanical properties. Among the various possible reactions, the following is known to be the most severe:

$$Al_2O_{3(s)} + TiC_{(s)} \longrightarrow Al_2O_{(g)} + TiO_{(g)} + CO_{(g)} \qquad (4.1)$$

The equilibrium partial pressure of CO for the above reaction is reported to be around 24 MPa (2.4×10^{-4}atm) at 2000 K and the consequent loss of weight during sintering of Al_2O_3-TiC composite is well known [2].

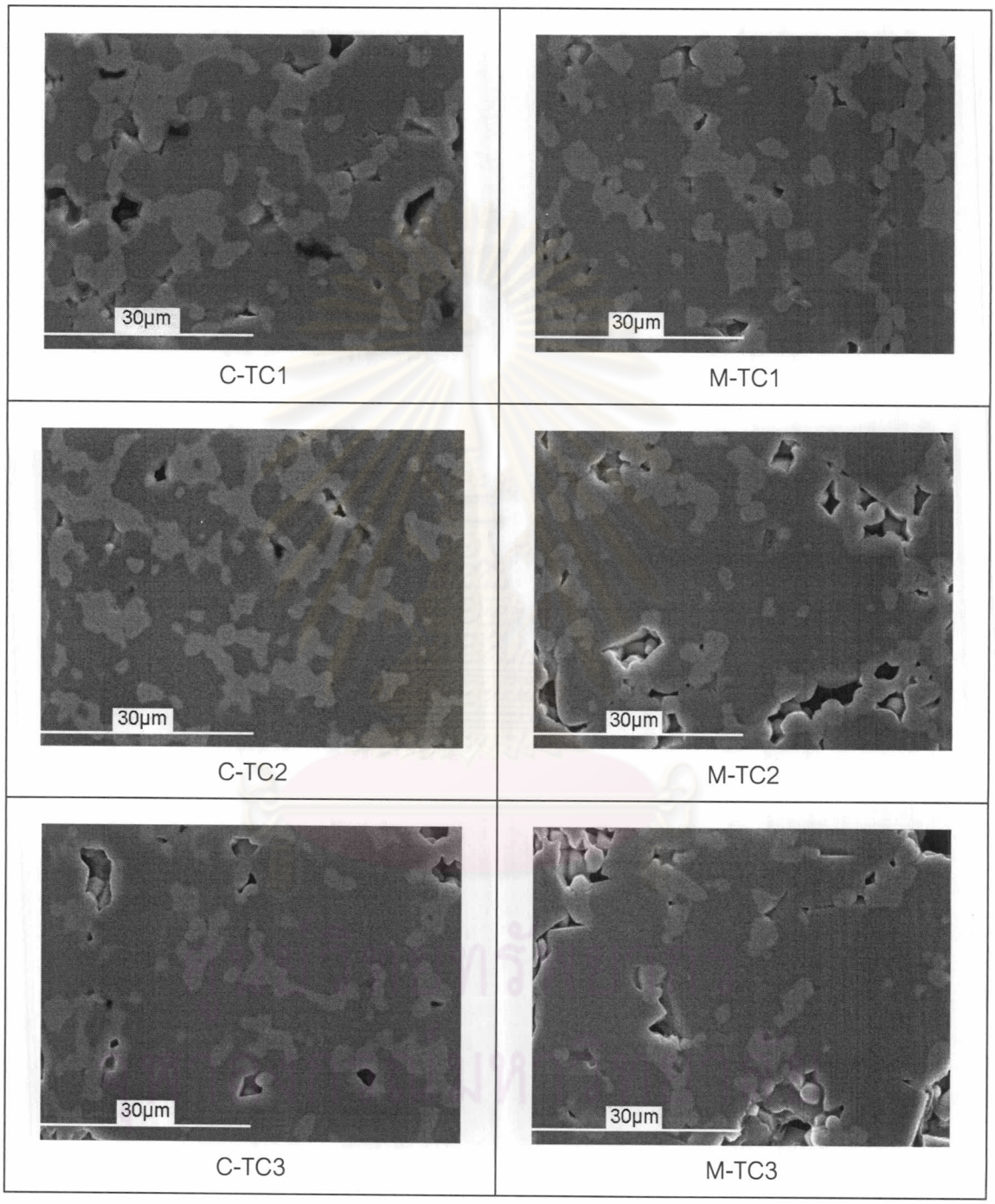

Fig. 4.13(a) SEM micrograph of conventional sintered products prepared form synthesized powders used rutile as titania precursor.

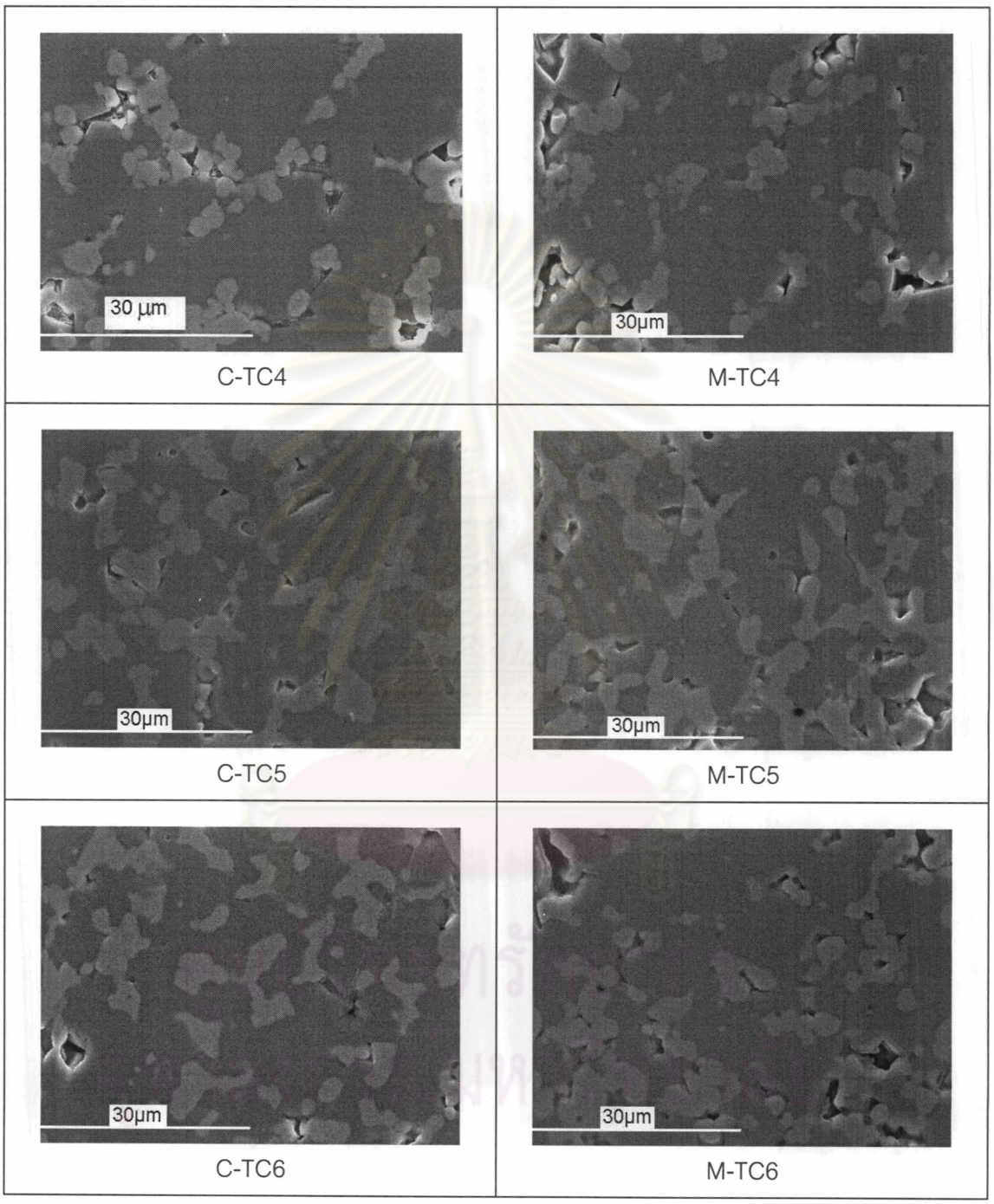

Fig. 4.13(b) SEM micrograph of conventional sintered products prepared form synthesized powders used anatase as titania precursor.

4.3.2 Conventional Sintering With Additive.

The role of additive which enhances the sintering ceramic materials can be related to change in surface energies, diffusivities, interfacial reactions, vapor pressures and solute diffusivities. For example, MgO is known as the sintering aids for Al_2O_3 ceramic, it can reduce grain growth during sintering [50]. The contribution of Y_2O_3 to changes in these properties is unknown for Al_2O_3-TiC composite. However, the study of K.W. Chae et al. [20] showed that 0.35wt% of Y_2O_3 can effectively inhibit the gas generation reaction. In this study, MgO and Y_2O_3 were thus used to minimize grain growth and reduce gas generation occurred during the sintering process of Al_2O_3-TiC composite as previously mentioned.

4.3.2.1 Determination of Sintering Temperature

The conventional synthesized TC1 powder (C-TC1) was selected to perform an experiment to determine the appropriate sintering temperature. According to relative density, apparent porosity and hardness depicted in Table 4.5, the best physical and mechanical properties of products was attained when sintered at 1800^{o}C. The corresponding microstructures illustrated in Fig. 4.14 were in good agreement with the physical properties of products. Although sintering products at 1700 ^{o}C provided a fine microstructure due to small grain growth, it also composes of large pores, which might not be able to densify. From this preliminary result, the sintering temperature of 1800^{o}C was then preferred for the sequential experiment to be discussed in the following section.

Table 4.5 Physical and mechanical properties comparison of Al_2O_3-TiC composite (C-TC1) at various sintering temperature.

Sintering temperature (^{o}C)	Relative density (%TD)	Apparent porosity (%)	Hardness (GPa)
1700	90.2	5.17	10.60
1800	95.6	0.21	15.04
1900 (undoped)	93.8	0.19	13.36

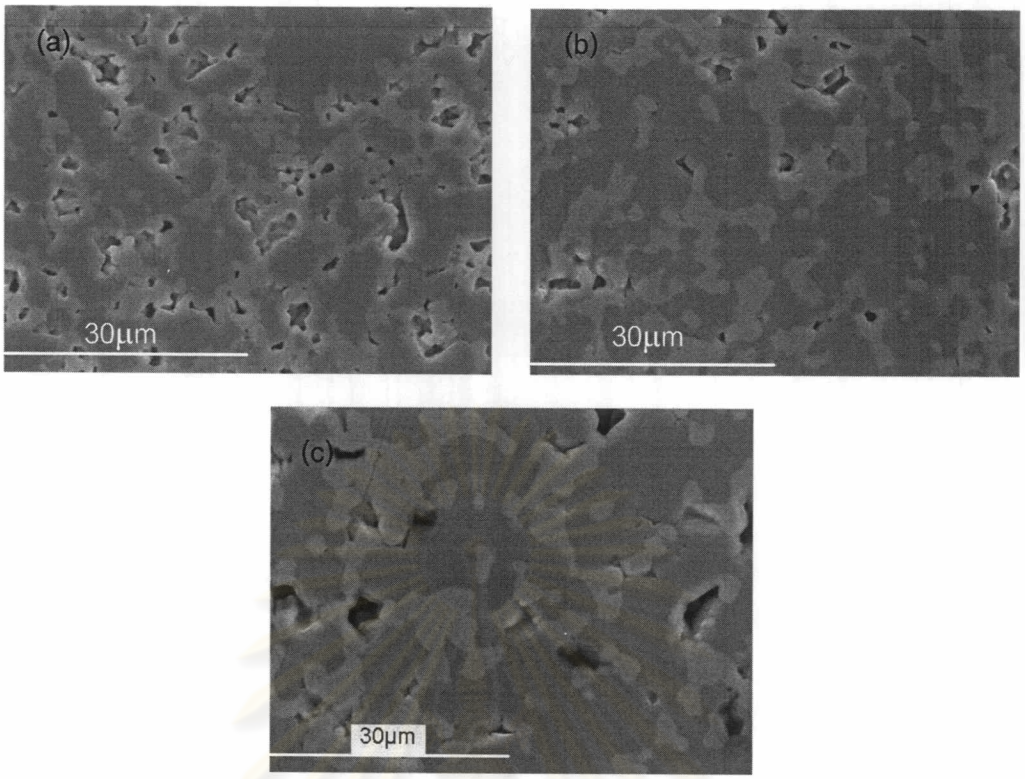

Fig. 4.14 SEM micrograph of C-TC1 sintered products with varying sintering temperatures (a)1700 ^{O}C (b) 1800 ^{O}C and (c) 1900^{O}C (undoped)

4.3.2.2 Physical Properties and Microstructures

Pressureless sintering at 1800^{O}C of Y_2O_3 and MgO-doped Al_2O_3- 47wt% TiC powders prepared by both microwave and conventional synthesis was investigated. Fig. 4.15 shows the relative densities of sintered products from various compositions at 1800^{O}C. It can be seen that the sintered density was improved although the sintering temperature was decreased. This indicated that not only lower temperature can reduce activation energy of gas release reaction but also the using of Y_2O_3 additive can effectively suppress chemical reaction between Al_2O_3 and TiC at higher temperature.

The relative densities of sintered products prepared from C-TC powders are in the range of 94.1 – 96.4 %TD while that prepared from M-TC powders are between 87.9 – 95.9 %TD. Comparing with the C-TC products, M-TC gave somewhat lower in densities, especially for the sintered product of M-TC3 powders; the apparent porosity and water absorbtion were also clearly higher as shown in Table 4.6. However, these physical properties of C-TC and M-TC sintered products in this case were not

much significantly different as what occurred in the sintered products at 1900°C, discussed earlier in previous section (4.3.1). Moreover M-TC1, M-TC2 and M-TC4 show the comparable density to the other corresponding C-TC products.

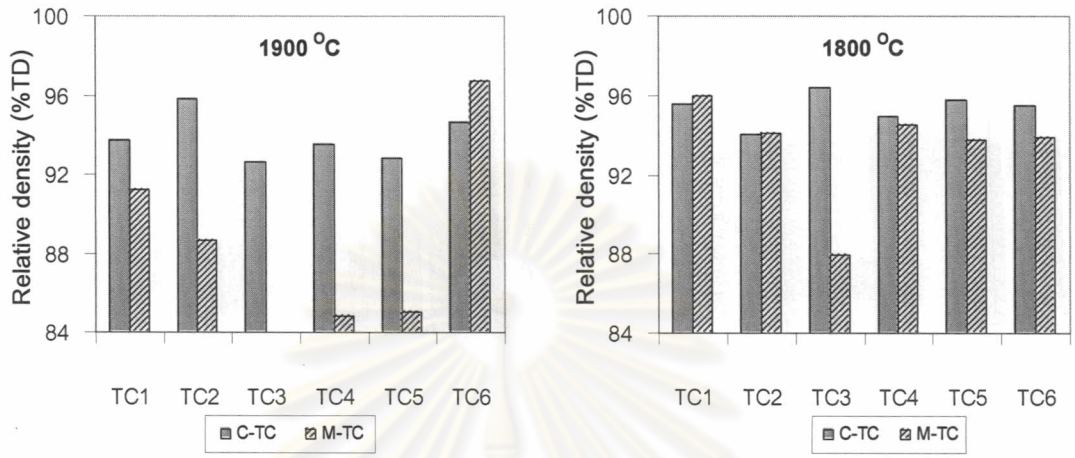

Fig. 4.15 Relative density of C-TC and M-TC products with sintering temperature of 1900°C (undoped) and 1800 °C (Y_2O_3 and MgO doped).

Table 4.6 Apparent porosity and water absorbtion of the Al_2O_3-TiC sintered products.

Compositions		TC1	TC2	TC3	TC4	TC5	TC6
Apparent porosity (%)	C-TC	0.21	0.25	0.12	0.17	0.16	0.30
	M-TC	1.43	0.87	9.26	0.58	0.85	1.08
Water absorbtion (%)	C-TC	0.05	0.06	0.23	0.04	0.04	0.07
	M-TC	0.34	0.21	2.40	0.14	0.21	0.26

The microstructures of theses composite are shown in Fig. 4.16. The EDS analysis was used to confirm that the dark phase is Al_2O_3 while light phase is TiC. The presence of SEM micrograph shows the consistent dispersion of Al_2O_3 and TiC phase. The TC3 and TC6 found low content of TiC phase which correspond to the phase conversion determination previously discussed in topic 4.2.3.2. The microstructures consist of mainly Al_2O_3 matrix and dispersed with a rather angular shaped TiC grain with a size of less than five microns. The larger interconnected grains of TiC was observed. Thus, the TiC particle size exhibited a somewhat large scatter. The samples are densified with mainly open porosity associated with the TiC particles and clusters. It

was found that grain size of each composition was affected from mean particle size of combusted powder (after milling process) which was shown in Table 4.3.

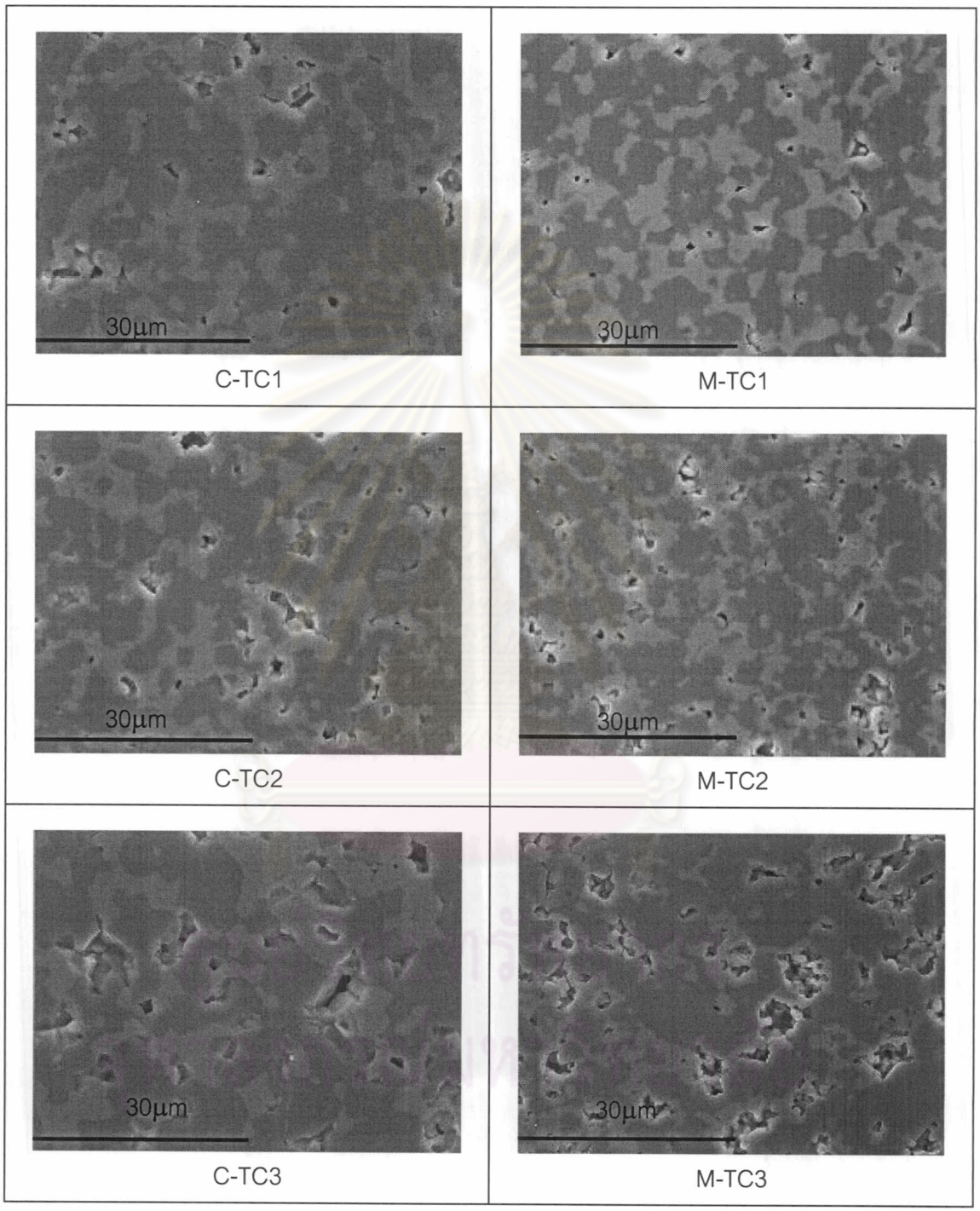

Fig. 4.16 (a) SEM micrographs of conventional sintered products at 1800^{o}C prepared form synthesized powders used rutile as titania precursor with MgO and Y_2O_3 doping.

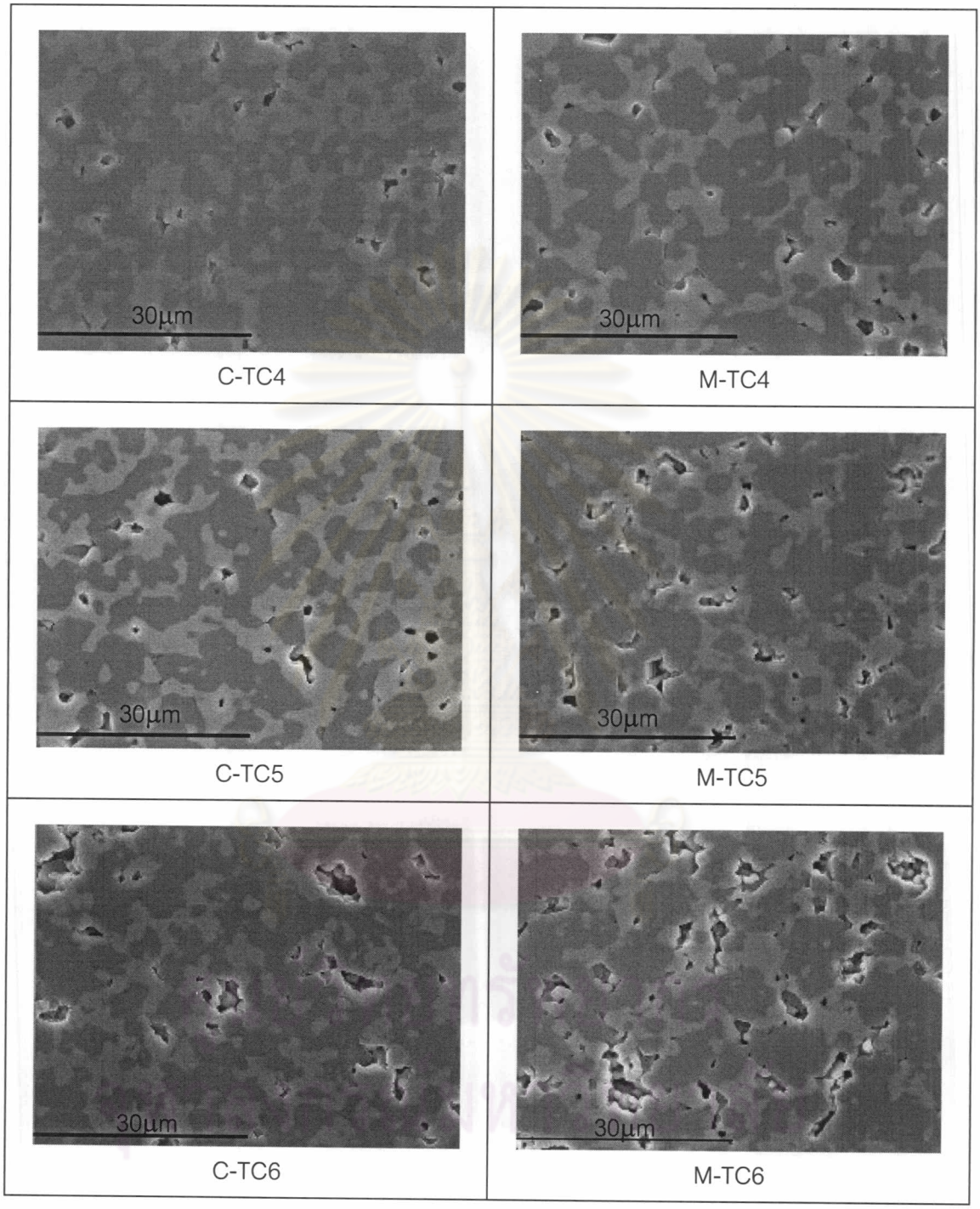

Fig. 4.16 (b) SEM micrographs of conventional sintered products at 1800°C prepared form synthesized powders used anatase as titania precursor with MgO and Y_2O_3 doping.

4.3.2.3 Mechanical Properties Investigation

The mechanical properties of sintered products are revealed in Table 4.7. The mechanical properties of C-TC products were superior as compared to M-TC product. However, there are some compositions of M-TC have a tendency to approach C-TC products, such as M-TC1, and M-TC5.

Table 4.7 Mechanical properties of the pressureless sintered products of Y_2O_3 and MgO – doped Al_2O_3-47wt%TiC powders prepared by combustion synthesis.

Compositions	Vickers hardness (GPa)		Fracture toughness ($MPa.m^{1/2}$)		Four-point bending (MPa)	
	C-TC	M-TC	C-TC	M-TC	C-TC	M-TC
TC1	15.0	14.2	4.35	5.19	368±52	321±45
TC2	14.1	12.7	4.95	4.30	423±44	284±37
TC3	13.4	7.0	5.23	7.79	405±31	225±72
TC4	14.6	13.3	4.56	4.95	425±32	227±51
TC5	15.7	13.1	4.00	4.46	443±29	295±68
TC6	9.9	9.0	9.17	7.99	426±44	365±55

The Vickers hardness seems to be related with relative density; the increase in relative density leads to high hardness products as seen in Fig.4.17. However this was not the case for the C-TC2, C-TC4 and M-TC5; the sintered products demonstrate good hardness though their density is not prominent. The report of Y.Wan et al. [16] suggested that the hardness increases with increasing TiC particle size. TiC has higher hardness than Al_2O_3, when it forms a connection and become coarser thus improve hardness of composites. The starting particle size of TiC powders for sintering process in the present study was very difficult to control since it was received from the violent exothermic combustion process. However, it can be observed in microstructure in Fig.4.17 (a) and (b) that the product with large cluster TiC and high connectivity correspond to the good hardness such as C-TC1, C-TC2, C-TC4, C-TC5, M-TC1 and M-TC4.

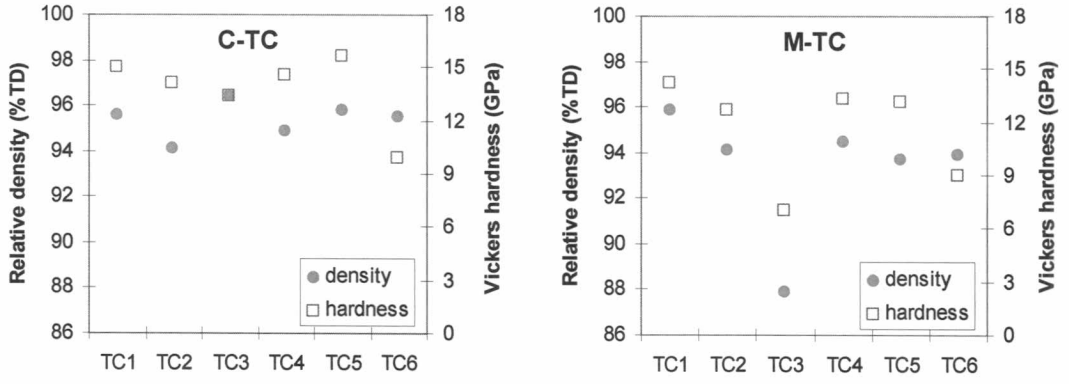

Fig. 4.17 The relative density and Vickers hardness of the Y_2O_3 and MgO – doped Al_2O_3-47wt%TiC composites prepared by combustion synthesis pressureless sintered at 1800°C.

There have been many studies concerning the toughness improvement in hard second-phase particle reinforced ceramics and two mechanisms are thought to be the particularly important in determining toughness: (1) crack deflection along weak grain boundaries and (2) crack trapping combined with crack face bridging by second-phase particle. However, the observations in this study revealed that both mechanisms seem not to play significant roles. The fracture morphology shows both intergranular and transgranular crack propagation characteristic as shown in Fig.4.18.

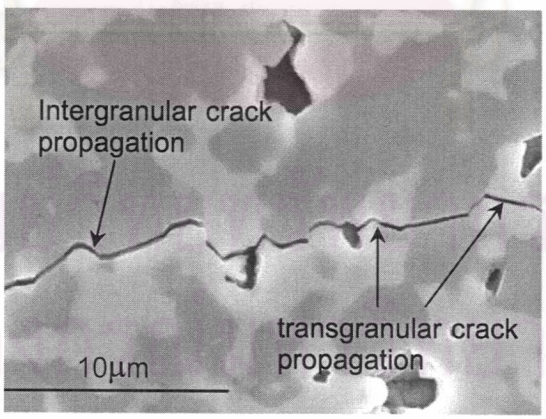

Fig. 4.18 Crack propagation characteristics in Al_2O_3-TiC composite (C-TC2)

When crack occurred in Al_2O_3 matrix it propagated along with interface between $Al_2O_3$and TiC phase, since crack tip intersecting the large TiC particle size and also interconnected grains, the crack would be collided and pinned rather than deflected, due to the intrinsic brittleness of TiC. This may be the reason that why no

deflecting or bridging were observed in some part of crack propagation. The transgranular crack propagated observation is in agreement with the result of J.Gong et al. [51] who observed the influence of TiC particle size on fracture toughness.

However, a possible explanation for improvement in toughness might be proposed by the difference between the linear coefficient of thermal expansion of Al_2O_3 ($7.4x10^{-6}$ $^oC^{-1}$) and TiC ($8.8x10^{-6}$ $^oC^{-1}$). This difference would result in residual stress developing within the composite. The compression field produced by TiC embedded in the Al_2O_3 matrix thus created resistance to the crack front propagation.

The fracture toughness of C-TC and M-TC, shown in Table 4.7, were comparable to or better than that reported by others presented in literature review (Table 2.5, Table 2.7 and Table 2.8). The C-TC6, M-TC3 and M-TC6 revealed remarkable better in fracture toughness. It was thought that a great number of open porosity of these products might be a primary cause. The crack propagation length in the testing products was shorten with these pores, then calculated to the high value of fracture toughness.

The four-point bending strength of C-TC was also higher than that of M-TC product. Typically, the bending strength was calculated from load applied at break point of sample. A surface defect, such as pore, of test specimens may affect on strength because it is the point of stress concentration and further originated crack. The apparent porosity of M-TC sample was obviously more than that of C-TC sample, thus lead to higher surface defect which is the weak point of test specimens.

4.3.2.4 Comparative Mechanical Properties with Literature

This section aims to the compare the physical and mechanical properties among the sintering studies of Al_2O_3-TiC combusted powder. The relative density and mechanical properties of C-TC products (except C-TC3 and C-TC6) and M-TC1 were approach to the ones which was reported by J.H.Lee et al [37] shown in Table 2.7, whereas their experiments were carried out at a higher sintering temperature (1890^oC) with the addition of the higher amount of MgO (0.8wt%). This implies that

sintering temperature and amount of additive play an important role on sintering behavior of Al_2O_3-TiC composite, therefore these parameters are needed to be investigated further to improve the sintering ability of combusted powder.

In addition, as compared to the properties report by R.A.Cutler [36] in Table 2.5, although their hardness was higher, the density and strength obtained in this study were comparable or superior. They proposed that the sintering ability of combusted powder is to be due to three factors: (1) the fine ultimate particle size of the combusted powder (approximately 0.1 – 0.5 μm), (2) free titanium (below detection by XRD) which acts as transient liquid phase above 1650^{o}C, and (3) free carbon which reduces a small amount of Al_2O_3 to form a transient liquid above 1850^{o}C. The starting particle size of their sintering process was smaller than the ones used in this present study, therefore it may be necessary to improve milling process to attain smaller starting particle size. Moreover the remained phase like free carbon and titanium which believed to assist the sintering ability of combusted powder was not found. However, XRD detected the Al-Ti-O metastable phase which may be affected to the sintering behavior; the further in-depth investigation is thus necessary.

In summary, the physical and mechanical properties of sintered microwave combusted powder were inferior as compared to the conventional ones. It might be a reason that conventional combustion took a longer time than microwave process. Therefore a liquid phase would probably present in the powder products for longer periods; thus densified Al_2O_3-47%TiC powders were obtained. Mechanical properties of sintered product can be controlled by its density and microstructure. High relative density and low apparent porosity resulted in good mechanical properties. The improvement of the hardness, fracture toughness and bending strength of composites can be manipulated by the TiC harder phase in term of initial particle size, distribution and also the ability to densify interconnected grain.

4.4 Part 3: Microwave Sintering

Preliminary experiment was performed to microwave sinter Al_2O_3-47wt%TiC combusted powders alone without susceptor. When TiC particle is dispersed in a microwave transparent Al_2O_3 matrix, despite the very low penetration depth (8 μm at room temperature) a large part of TiC mass may suscept with microwave thus the composites can be heated to higher temperature. The highest temperature that the sample experienced was at only 894°C. This result suggests that this Al_2O_3-47wt%TiC composition may not contain enough TiC for fast heating even under microwave power of 2.4kW. Also heat loss may still occur since the size of alumina insulation board surrounded sample is not small enough. The heated sample was fragmented from center into pieces. This implied that an inverse temperature profile was developed, where the inside of sample is hotter than the surface, as compared to conventional radiant heating where the highest temperature would be found on the surface of the sample.

4.4.1 Microwave heating profile

Microwave hybrid heating (MHH) of Al_2O_3-47wt%TiC were then performed. SiC susceptor was used as a secondary heat source providing assistance for materials that heat slowly by microwave energy and also reduce the temperature gradients thus promote more uniform heating. Thus, sample cracking was not found. At the beginning of sintering, heat is generated in the interior of sample by TiC and is provided on the exterior of sample by SiC. As the temperature of the sample increases to a point where Al_2O_3 has high enough dielectric loss to couple directly with field, it then absorbs microwave energy and turn into heat.

Experiments were carried out to find an appropriate thermal package for sintering microwave combusted powder product at a maximum temperature of 1700°C. Fig. 4.19 shows a comparison of temperature profiles resulted from the microwave sintering of synthesized TC1-powders using the two different SiC susceptor setup.

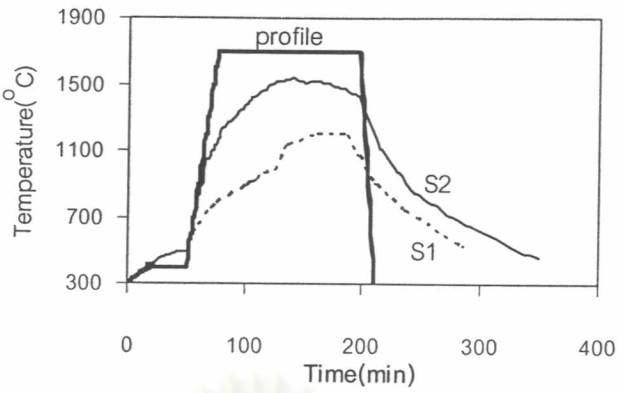

Fig.4.19 Microwave temperature-time profiles obtained from S1- and S2- susceptor setups.

A setup of S1 is where a disc sample was placed on a center of 26g-round plate SiC and surrounded with 8 pieces of thin curve SiC which weigh approximately 20 g each. The sample package was then enclosed in an insulation board before sintering. A setup of S2 is where a disc sample embedded in a 150g - SiC particles with a size range in between 0.5 - 1 mm. It can be seen that there is a distinctly different heating behavior for these susceptor setups, as the difference in slope of these two curves indicates. S2 setup exhibited a markedly higher heating rate than S1 under a given sintering condition, even though the total mass of S1 (186 g) was more than S2 (150 g). The sample sintered under S2 setup reached a temperature of 1100^{o}C within 50 min while it took S1 setup for 2hr to attain the same sintering temperature. The maximum sintering temperature was about 1200^{o}C in the case of S1, compared with 1500^{o}C in the case of S2 setup. The explanation was thought to be because a higher mass of 186g-S1 SiC susceptor competed with TiC for microwave energy more excessively as compared to 150g-S2 SiC, thus heat generated internally within sample itself decreased. In addition, in S2 setup, heat generated from SiC particles can be easily conduct to sample compact as they are in close contact to each other, thus minimizing the heat loss to the environment. When the susceptor are used in many separate parts (S1), heat loss occurs more easily as it radiates and conducts to sample surface. Therefore, it was more difficult to raise the sintering temperature over 1200^{o}C under S1 setup without an increasing in the microwave power.

4.4.2 Physical Properties of microwave sintered Products

Fig. 4.20 illustrates a sintering curve for microwave and pressureless sintering of Al_2O_3 - TiC powders prepared by microwave combustion synthesis in terms of sintered density vs. temperature.

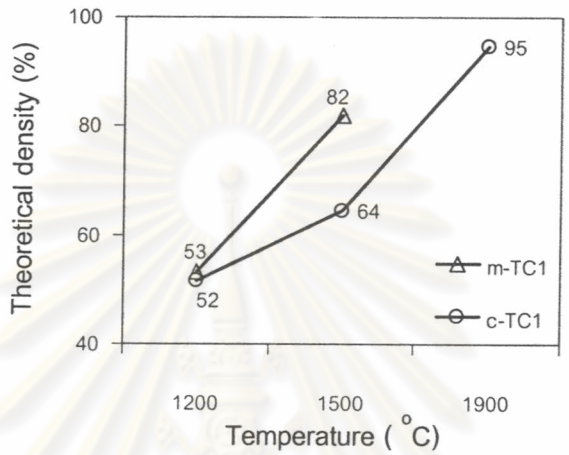

Fig. 4.20 Density versus temperature of microwave and conventional firing.

At 1200°C the density of microwave firing sample were comparable to those of conventional firing. As the sintering temperature increases up to 1500°C, the microwave sintered density increased from 53% to 82% of the theoretical density (TD) indicating the intermediate stage of sintering. This temperature was significantly lower than that required for pressureless sintered sample to obtain the same density (~1700°C). It is expected that this trend may continue at higher temperature to obtain a nearly full densification of Al_2O_3-TiC composites at lower temperature than conventional sintering, normally in range of 1800 - 2000 °C. However, it will be necessary to modify a new thermal package to minimize the energy loss and insulation volume. Susceptor configuration is also need to be adjusted in order to start fast heating of sample efficiently.

The linear shrinkage in thickness and diameter of sintered sample is in good agreement with the result of density. It can be seen in Table 4.8 that the

microwave sintered product shrink slightly more than conventional one at 1200°C. However, as sintering temperature increases up to 1500°C, the shrinkage of microwave sintered products are manifestly exceed those of conventional sintered samples at almost 100%. Also, this shrinkage value (13.95-14.06%) was not far from one obtained from conventional sintered at 1900°C.

Table 4.8 Percent shrinkage at various sintering temperatures of microwave and conventional sintering

Temperature (°C)	Process	Shrinkage (%)	
		Diameter	Thickness
1200	microwave	2.95	2.27
	conventional	2.10	1.94
1500	microwave	13.95	14.06
	conventional	7.72	7.96
1900	conventional	17.81	17.21

4.4.3 Microstructure of microwave sintered Products

The higher in density and shrinkage of microwave sintered composites at a given temperature was confirmed by SEM micrographs shown in Fig.4.21. At 1200°C, it can be observed that the morphology of conventional sintered product (Fig.4.21b) was not so much different from green compact, while some particles in microwave sintered sample (Fig.4.21a) began to melt and bond with each other. The neck size ratio and shrinkage were both small and the grain size was no larger than the initial particle size. As temperature increased to 1500°C, the conventional sintered samples developed an interparticle necking as its density increased from 52% to 64%, the latter portion of the initial stage of sintering (Fig.4.21d). The pore structure is open and fully interconnected. On the other hand, Fig.4.21c shows that the microwave sintered samples at 1500°C seems to be in an intermediate stage of sintering. Grain boundaries formed at the contacts while grain size seemed larger than initial particle size and porosity also decreased.

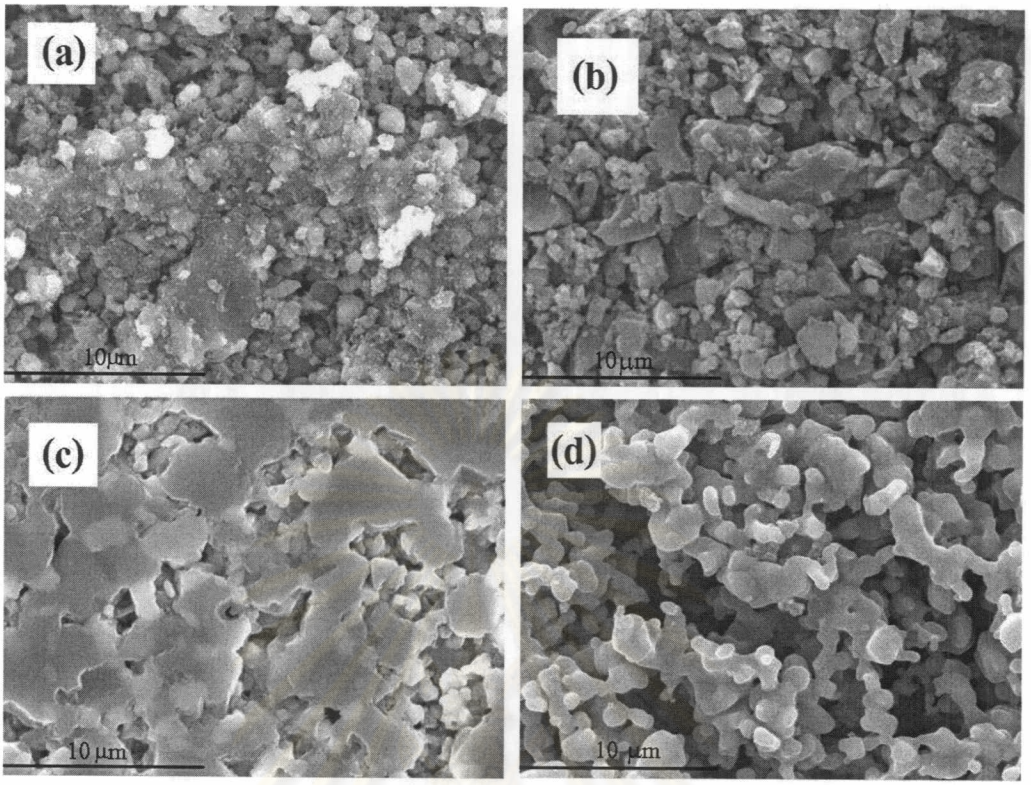

Fig.4.21SEM of product surface: (a) microwave sintering at 1200^{o}C (b) conventional sintering at 1200^{o}C (c) microwave sintering at 1500^{o}C and (d) conventional sintering at 1500^{o}C.

In case of conventional sintering, EDS analysis showed the remained TiC phase only. The possible reason might be because of gas-generating from the reaction between Al_2O_3 and either free carbon or combined carbon in TiC at high temperature that was known to be detrimental to densification. This situation was not taking place in microwave product; it was thought that fast sintering process and short dwelling time were present in microwave process.

In conclusion, the highest density microwave sintered sample, prepared from microwave combusted powders, achieved was 82%TD at 1500°C under 2.4kW. The microwave sintered sample had a tendency to obtain a nearly full densification at lower temperature compared to conventional process. Moreover, the gas-generating from reaction between Al_2O_3 and TiC can be suppressed in microwave sintering process due to fast sintering and short dwelling time. The development of an appropriated

thermal package for sintering in microwave energy is critical. A susceptor mass sufficient to start fast firing and minimizing the refractory volume and energy loss are of great concerns.